

## Effect of scattering on zero-bias anomaly and conductance reduction in quasi-one-dimensional quantum wires

K. M. Liu,<sup>1</sup> V. Umansky,<sup>2</sup> and S. Y. Hsu<sup>1</sup><sup>1</sup>*Department of Electrophysics, National Chiao Tung University, Hsinchu 30010, Taiwan*<sup>2</sup>*Braun Center for Submicron Research, Weizmann Institute of Science, Rehovot 76100, Israel*

(Received 4 September 2009; revised manuscript received 9 January 2010; published 11 June 2010)

We present a systematic study on the zero-bias conductance peak and its dependences on the carrier density and structural geometry in quasi-one-dimensional quantum wires (QWs). This zero-bias anomaly (ZBA) is suppressed by either decreasing the carrier density or increasing the QW length. The differential conductance at zero bias decreases with increasing temperature in accordance with a thermal-activation model up to a well-defined cut-off temperature. We demonstrate that the activation energy, cut-off temperature, and width of the ZBA are correlated, and suggest that these features are controlled by electron scattering in QWs.

DOI: [10.1103/PhysRevB.81.235316](https://doi.org/10.1103/PhysRevB.81.235316)

PACS number(s): 73.21.Hb, 73.23.Ad, 72.10.Di

### I. INTRODUCTION

In a ballistic quasi-one-dimensional (1D) channel, the linear conductance is quantized into integer multiples of  $G_0 = 2e^2/h$  due to the transmission of spin-degenerate 1D subbands within a noninteracting electron picture.<sup>1,2</sup> Peculiar phenomena, however, such as a 0.7 anomaly and a zero-bias anomaly (ZBA), referred to as the conductance peak centered at zero bias in source-drain bias spectroscopy, are often observed near the first quantization plateau and have attracted much attention.<sup>3,4</sup> The 0.7 anomaly which usually accompanies a conductance reduction near the first plateau, a lowered conductance at high temperatures, was mostly attributed to spin-related mechanisms.<sup>4–20</sup> One-dimensional Kondo physics was proposed to describe the experimental findings, such as the scaling of conductance to a modified Kondo form and the splitting of a zero-bias conductance peak in a parallel magnetic field.<sup>4,17–20</sup> More recently, however, others have claimed that 1D Kondo physics does not fully explain the intricate behaviors of the ZBA.<sup>21–23</sup> In some devices, the splitting of a zero-bias conductance peak is absent in magnetic fields as high as 10 T and at  $G < 0.5G_0$ , where the channel is fully spin-polarized.<sup>22</sup> In a few devices, splitting occurs in magnetic fields but two split peaks can resolve back into a single peak by *laterally shifting* the quantum wire (QW).<sup>22,23</sup> Additionally, zero-bias conductance peak splitting is almost linearly dependent on the split gate voltage.<sup>23</sup> These findings indicate that ZBA cannot be explained by Kondo physics. Thus, the issue is not yet completely clarified and a comprehensive understanding requires further study.

A lateral shift of the QW by electrical means changes the microscopic electric field. This raises an interesting question: how and why is the ZBA influenced by the physical properties of the QW, such as width, length, or carrier density? Studies of this issue may shed light on the formation of ZBA at low temperatures as well as the conductance reduction. Recently, it was reported that backscattering in QWs can be controlled by tuning a nonuniform local potential through side gates, implying that electron scattering is sensitive to the details of the potential profile.<sup>24</sup>

Here, we focus on the source-drain bias spectroscopy and temperature-dependent differential conductance at zero bias

in the range of  $G < G_0$ . QWs of various channel lengths and carrier densities are studied. The ZBA is suppressed by either increasing the channel length or decreasing the electron density. The temperature dependence of differential conductance at zero bias follows closely the thermal-activation behavior below the cut-off temperature. In addition, we found a correlation between the activation temperature, cut-off temperature, and ZBA width. The results indicate that the conductance reductions at finite temperatures and finite biases are affected similarly by the same physics. We suggest that electron scattering plays a dominant role in both ZBA and temperature-dependent conductance.

### II. EXPERIMENTAL SPECIFICATIONS

The two-dimensional electron gas (2DEG) that forms at the interface of a GaAs/Al<sub>x</sub>Ga<sub>1-x</sub>As heterostructure was grown using molecular beam epitaxy at the Weizmann Institute in Israel. Shubnikov-de Haas and Hall measurements were used to determine the areal electron density  $n$ . Mobility is approximately  $1.7 \times 10^6$  cm<sup>2</sup>/Vs and  $n$  is  $2.4 \times 10^{11}$  cm<sup>-2</sup> corresponding to the elastic mean-free path  $\ell$  of  $\sim 14$   $\mu$ m at low temperatures. Electron beam lithography along with thermal deposition were used to fabricate metallic gates on (100) plane of the substrate. A quasi-one-dimensional quantum wire can be formed by depleting the 2DEG  $\sim 93$  nm beneath the negatively biased split gates pair. The length of our QWs ranges from quasizero to 5  $\mu$ m while the nominal gap width is kept constant at  $\sim 0.45$   $\mu$ m. A metallic top gate (tp) was fabricated on top of the split gates, isolated by a  $\sim 100$ -nm-thick dielectric layer of cross-linked polymethylmethacrylate, to control the carrier concentration. Measurements were performed mainly in a pumped <sup>3</sup>He cryostat and occasionally in a dilution refrigerator with base temperatures of 0.27 K and 40 mK, respectively. Differential conductance measurement was carried out using a standard four probes ac lock-in technique at 51 Hz with a small excitation voltage of 10  $\mu$ V.

### III. RESULTS AND DISCUSSION

When a negative voltage is applied to a pair of split gates, the potential depletes the 2DEG to form a 1D channel result-

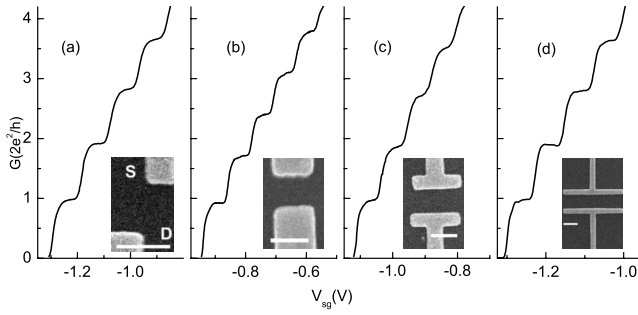


FIG. 1.  $G(V_{sg})$  and micrographs of QWs of various lengths: (a) quasizero, (b)  $0.5 \mu\text{m}$ , (c)  $0.8 \mu\text{m}$ , and (d)  $2 \mu\text{m}$ . The scale bars (white bars in the insets) indicate a length of  $0.5 \mu\text{m}$ . The top gate is grounded for all four data sets.

ing in a typical quantized conductance. Conductance versus split gate voltage of four samples with different QW lengths, quasizero,  $0.5$ ,  $0.8$ , and  $2 \mu\text{m}$ , are plotted in Fig. 1, revealing that there are conductance plateaus due to the transmission of 1D subbands for QWs. The plateaus can be aligned exactly to the integer multiples of  $G_0$  by subtracting the series resistance of bulk 2DEG from the data, such as in Ref. 25 by Thomas *et al.* Here, we present the raw data since the series resistance does not affect our results. For QWs of various lengths, quantized plateaus are well developed for  $L \leq 2 \mu\text{m}$ , implying that the mean-free path is much longer than the channel length. For a  $L=5 \mu\text{m}$  QW, the quantization steps remain the same, but the quantized conductance is lower compared with the  $L \leq 2 \mu\text{m}$  QWs, indicating that the QW is slightly diffusive. The presented transport for QWs with lengths less than  $2 \mu\text{m}$  is indeed within the ballistic regime. Occasionally, charges can be trapped in samples during the cooling process and serve as extra scatterers to degrade conductance plateaus. This would not apply, however, to our work. The systematic behaviors reported here were obtained from 13 samples through many thermal cycles. It should be noted that transport behaviors depend on the geometry of the QW inside but not outside of the channel. For example, no significant difference is noted between the T-bar and straight-bar split gates. This is reasonable because the depletion regions isolate a confined QW from the 2D electron sea.

Electron transport is sensitive to carrier density, which can be effectively tuned by biasing the top gate voltage  $V_{tp}$  in the heterostructures, in either 1D or 2D.<sup>26</sup> Our previous work on transconductance spectroscopy, which is referred to as the half-plateau method, showed that carrier density is effectively changed by tuning  $V_{tp}$ .<sup>27</sup> In Figs. 2(a)–2(c), three conductance traces for a  $L=0.5 \mu\text{m}$  QW with  $V_{tp}=+0.4$ ,  $-0.1$ , and  $-1.45 \text{ V}$  at  $T=0.3 \text{ K}$  are shown as black lines. The threshold  $V_{sg}$  of the pinch-off voltage becomes less negative from left to right, implying that carrier density is decreased with decreasing  $V_{tp}$ . Once the carrier density is substantially reduced, the quantized plateaus disappear while a quasisoulder appears at  $\sim 0.5G_0$  [Fig. 2(c)]. Some corresponding conductance traces at different temperatures are also plotted in Figs. 2(a)–2(c). Both Figs. 2(a) and 2(b) show that when temperature is increased from  $0.3$  to  $4.2 \text{ K}$  conductance decreases in the vicinity of the first plateau. A quasisoulder

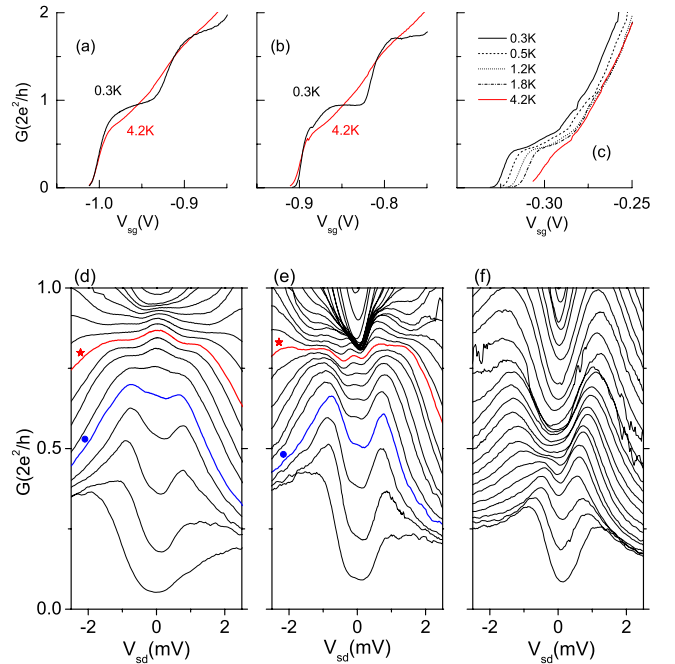


FIG. 2. (Color online) [(a)–(c)] Zero-bias differential conductance versus split gate voltage of a  $L=0.5 \mu\text{m}$  QW for  $V_{tp}=(a)$   $+0.4 \text{ V}$ , (b)  $-0.1 \text{ V}$ , and (c)  $-1.45 \text{ V}$ , respectively, at various temperatures. [(d)–(f)] Source-drain bias spectroscopies of the same sample at the same top gate voltages at  $0.3 \text{ K}$ . (d)  $V_{tp}=+0.4 \text{ V}$ .  $V_{sg}$  is from  $-938$  to  $-1002 \text{ mV}$  in  $4 \text{ mV}$  steps. Star- (red) and dot- (blue) labeled traces indicate  $V_{sg}=-970$  and  $-986 \text{ mV}$ , respectively. (e)  $V_{tp}=-0.1 \text{ V}$ .  $V_{sg}$  is from  $-819$  to  $-900 \text{ mV}$  in  $3 \text{ mV}$  steps. Star- (red) and dot- (blue) labeled traces indicate  $V_{sg}=-873 \text{ mV}$  and  $-891 \text{ mV}$ , respectively. (f)  $V_{tp}=-1.45 \text{ V}$ .  $V_{sg}$  is from  $-280$  to  $-324 \text{ mV}$  (top to bottom) in  $2 \text{ mV}$  steps.

forms near  $0.7G_0$  while the plateaus are washed out. The phenomenon is a typical feature of the  $0.7$  anomaly.<sup>4</sup> For the same QW with more negative  $V_{tp}$  in Fig. 2(c), conductance traces at different temperatures remain almost the same. Notice that the curves of higher temperatures are horizontally shifted for clarity in Fig. 2(c). As expected, conductance is not sensitive to temperature in the sample with low carrier density while a clear temperature-induced conductance reduction around  $0.7G_0$  occurs in the sample with high carrier density.<sup>25</sup>

We investigated the source-drain bias spectroscopy by sweeping a dc source-drain voltage  $V_{sd}$  across a confined QW and measuring the differential conductance  $G=dI/dV_{sd}$ . Figures 2(d)–2(f) show the spectroscopies  $G(V_{sd})$  against  $V_{sg}$  of this sample for the three identical top gate voltages at  $T=0.3 \text{ K}$ . For  $V_{tp}=+0.4 \text{ V}$  in Fig. 2(d), the differential conductance exhibits clearly a series of single peak centered at  $V_{sd}=0$  for  $G < G_0$  referring to as ZBA, e.g., the star-labeled and the neighboring curves. The feature is novel and distinguishable from the bell-shaped structure of the nonlinear conductance of the transmission of the subbands.<sup>28</sup> Based on the source-drain bias spectroscopies of numerous samples at a series of  $V_{tp}$ , ZBA becomes weaker with decreasing carrier density. Specifically, the ZBA at  $V_{tp}=-0.1 \text{ V}$  [Fig. 2(e)] is narrower than at  $V_{tp}=+0.4 \text{ V}$  [Fig. 2(d)], and disappears en-

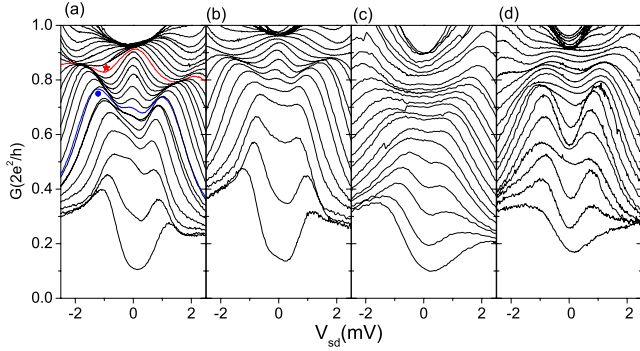


FIG. 3. (Color online) Source-drain bias spectroscopies of QWs of several lengths at 0.3 K for  $V_{tp}=0$ . (a)  $L$ =quasizero. From top to bottom,  $V_{sg}$  decreases from  $-1450$  to  $-1558$  mV in 4 mV steps. Star- and dot-labeled traces indicate  $V_{sg}=-1498$  (red) and  $-1526$  mV (blue), respectively. (b)  $L=0.25$   $\mu\text{m}$ .  $V_{sg}$  is from  $-914$  to  $-1002$  mV in 4 mV steps. (c)  $L=0.8$   $\mu\text{m}$ .  $V_{sg}$  is from  $-570$  to  $-612$  mV in 2 mV steps. (d)  $L=2$   $\mu\text{m}$ .  $V_{sg}$  is from  $-810$  to  $-858$  mV in 2 mV steps.

tirely at  $V_{tp}=-1.45$  V [Fig. 2(f)]. We characterize the width of a ZBA by  $\Delta V_{sd}^{ZBA}$ , the source-drain voltage difference between the “peak” and the “bottom” of the ZBA. From the star-labeled curve to the dot-labeled curve in Fig. 2(d),  $\Delta V_{sd}^{ZBA}$  decreases from  $\sim 750$  to  $\sim 280$   $\mu\text{V}$  with decreasing  $V_{sg}$ . Beyond the dot-labeled curve, the ZBA is absent for  $V_{sg} < -986$  mV. Similar trend holds in Fig. 2(e). The width drops from  $\sim 250$   $\mu\text{V}$  (the star-labeled curve) to  $\sim 160$   $\mu\text{V}$  (the dot-labeled curve) and the ZBA disappears for  $V_{sg} < -891$  mV. As to the sample with the lowest carrier density in Fig. 2(f), no ZBA is present for all split gate voltages. The observations evidence that ZBA is suppressed by decreasing the carrier density.

A robust 0.7 anomaly along with the absence of ZBA in ultralow-disordered QWs was reported by Reilly *et al.*<sup>12</sup> They suggested that carrier-density-induced enhancement in spin-splitting results in a spin gap.<sup>12</sup> Our observation of the systematic evolution of ZBA with respect to carrier density inspires an alternative thought. From electron-electron interaction (EEI) perspective, a system of lower carrier density has, in general, stronger EEI. It was well established that EEI contributes a Coulomb anomaly in the density of states which brings about a tunneling conductance gap at  $T=0$  and a negative tunneling conductance cusp at finite temperatures.<sup>29,30</sup> This could suppress the ZBA in a low carrier density QW. One would expect that the ZBA depends on QW geometry which affects EEI. To investigate the influence of QW length on the effect, we systematically studied the source-drain bias spectroscopies of QWs with quasizero  $\leq L \leq 5$   $\mu\text{m}$ .

The results presented in Fig. 2 imply that there will be a weak but nonzero ZBA for a  $L=0.5$   $\mu\text{m}$  QW at  $V_{tp}=0$  V. Here, we present  $G(V_{sd})$  against  $V_{sg}$  for other four samples with  $L$ =quasizero, 0.25, 0.8, and 2  $\mu\text{m}$ , at  $V_{tp}=0$  and  $T=0.3$  K in Fig. 3. The  $L$ =quasizero QW has a very strong ZBA. In Fig. 3(a),  $\Delta V_{sd}^{ZBA}$  decreases from  $\sim 1.2$  mV (the star-labeled curve) to  $\sim 290$   $\mu\text{V}$  (the dot-labeled curve) with decreasing  $V_{sg}$ . The  $L=0.25$   $\mu\text{m}$  QW has a slightly weaker

ZBA [Fig. 3(b)]. Both QWs have a relatively wider and taller conductance peak in their spectroscopy curves compared with the  $L=0.5$   $\mu\text{m}$  QW (Fig. 2). ZBA completely disappears in the other two QWs of  $L=0.8$  and 2  $\mu\text{m}$  shown in Figs. 3(c) and 3(d). The same result is observed in other QWs of various lengths ranging from 0.8 to 5  $\mu\text{m}$ . Therefore, the ZBA is suppressed by increasing QW length. These data are not consistent with Koop *et al.*,<sup>31</sup> who reported no length dependence of ZBA for QWs ranging in length from 0.1 to 0.45  $\mu\text{m}$ . It is slightly difficult to distinguish the difference in ZBA among our QWs in the range of 0.2–0.5  $\mu\text{m}$ . By also including the data for the quasizero and longer QWs, however, we provide a full picture of the evolution of ZBA with respect to QW length. The  $L \leq 2$   $\mu\text{m}$  QWs are at least a few times shorter than the mean-free path and hence, the diffusive scattering is negligible. In all of these samples, the differential conductance traces at zero-bias demonstrated many clear quantized conductance plateaus. There is neither superimposed resonance peak nor distorted plateau in  $G(V_{sg})$ . This feature is robust to thermal cycling, indicating that the ballistic transport is not affected. It has been suggested that spin polarization can be enhanced in long QWs to split the ZBA.<sup>8,11</sup> In our long QWs, we did not observe any splitting of the zero-bias conductance peak. We suggest that the increase in QW length allows for additional scattering of conducting electrons, which results in enhanced EEI and correspondingly, a diminished ZBA. For the  $L=5$   $\mu\text{m}$  QW, the lowered quantized conductance could be attributed to diffusive scattering. As the conductance quantization is sustained, however, the transport is mostly ballistic. In this case, we believe that the increased channel length still plays a dominant role in suppressing ZBA.

One more interesting phenomenon is that ZBA seems to be accompanied by a temperature-induced conductance reduction for  $G < G_0$ . Figure 2 shows the representing behavior for all other samples in the study of carrier density effect. Here, we determine if there is a correlation between the ZBA and the temperature-induced conductance reduction. We plot three  $G(T)$  traces of a  $L$ =quasizero QW in the inset of Fig. 4(a) to show the typical temperature-dependent conductance behavior. The zero-bias differential conductance decreases with increasing temperature. Although temperature dependence of the 0.7 anomaly has been intensively studied for quite some time, the results vary widely.<sup>4,21,22,32,33</sup> Among them two types were mostly proposed, Kondo-type,<sup>4</sup> and activated temperature-dependent behaviors.<sup>21,22,32,33</sup> Numerical fittings using both Kondo-type<sup>4</sup> and thermal-activation models to the data are shown as dashed and solid lines in the inset of Fig. 4(a), respectively.<sup>34</sup> Both models seem to describe experimental results well at low temperatures. The applicable temperature range, however, is wider and the fitting parameters obtained from the fit exhibit a systematic variation in the activation model. Hence, we adopted the activation model to analyze the data.

The temperature-dependent conductance based on the thermal-activation model is expressed as  $G(T)=G(0)(1-Ce^{-T_a/T})$  where  $G(0)$  is the measured conductance at the base temperature.  $T_a$  and  $C$  are the fitting parameters.<sup>32</sup> Rearranging the equation,  $f_a$  defined as  $\frac{1}{C}[1-\frac{G(T)}{G(0)}]$  equals  $e^{-T_a/T}$ . Semilogarithmic plots of  $f_a$  versus  $T_a/T$  for a  $L$ =quasizero

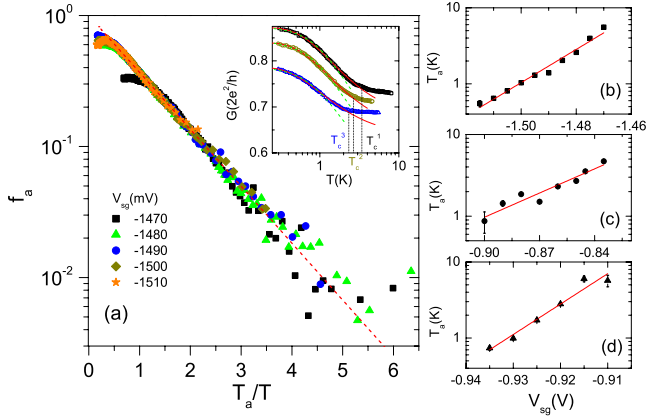


FIG. 4. (Color online) (a) Semilogarithmic plot of  $f_a$  vs  $T_a/T$  for a  $L$ =quasizero QW against a series of  $V_{sg}$  at  $V_{tp}=0$ . (see text) The dashed line is the least-square-root linear fit. Inset: three typical traces of measured  $G(T)$ , along with the simulated curves of the activation model (solid lines) and Kondo-type model (dashed lines) (Ref. 34). The cut-off temperature at which  $G(T)$  deviates from activation behavior is located and indexed as  $T_c^i$  for a split gate voltage  $V_{sg}^i$ . [(b)–(d)] Activation temperature vs split gate voltage at  $V_{tp}=0$  for (b) and (c) two  $L$ =quasizero QWs and (d) a  $L=0.5 \mu\text{m}$  QW. Lines were fitted using the linear least-square-root regression method.

QW against a series of  $V_{sg}$  at  $V_{tp}=0$  are presented in Fig. 4(a) to confirm the typical thermal-activation behavior. After scaling  $T$  by  $T_a$  in this semilogarithmic Arrhenius plot, all traces generally collapse onto a universal curve following a linear relation down to  $\sim 0.2T_a$  ( $T_a/T \sim 5$ ). The dashed line is the least-square-root linear fit. Thermal-activation behavior is valid up to a “cut-off” temperature,  $T_c$ . In Fig. 4(a), traces of  $f_a$  show a downward trend deviating from the linear fit at low values of  $T_a/T$ .  $T_c$  was determined by finding the temperature at which the data begins to deviate from the fit. As an example,  $T_c$  for three  $V_{sg}$  is labeled in the inset of Fig. 4(a). The evolution of  $T_c$  with respect to either  $V_{sg}$  or  $G(0)$  is obtained for  $G < G_o$ . As  $G(0)$  decreases,  $T_c$  decreases and so does  $T_a$ .  $T_a$  increases with increasing  $V_{sg}$  from sub-Kelvin for  $G(0) \sim 0.5G_o$ , to a few Kelvin in the vicinity of the first plateau. The activation temperature, as a function of  $V_{sg}$  for three samples, is shown in Figs. 4(b)–4(d). Other samples, except those with either low carrier density or long channel length, exhibit similar behavior with an exponential dependence of the activation energy on split gate voltage, which is consistent with previous experimental findings by other groups.<sup>21,22</sup> Bruus *et al.*<sup>33</sup> proposed that the observed activated behavior in  $G$  is related to the thermal depopulation of a subband with a gate-voltage-dependent subband edge. The power-law relation between the activation energy and split gate voltage was experimentally obtained by Bruus *et al.*<sup>32,33</sup>

It is quite interesting that there is not only a correlation between  $T_a$  and  $T_c$ , but also a close relation between  $T_a$  or  $T_c$  and the ZBA width for  $G \leq 0.9G_o$ . The relations can be clearly demonstrated by scaling  $[G(0), T_c]$ ,  $[G(0), T_a]$  extracted from the temperature-dependent conductance, and  $(G_{peak}^{ZBA}, \Delta V_{sd}^{ZBA})$  extracted from the source-drain bias spectroscopy on the same plot as shown in Figs. 5(a) and 5(b) for

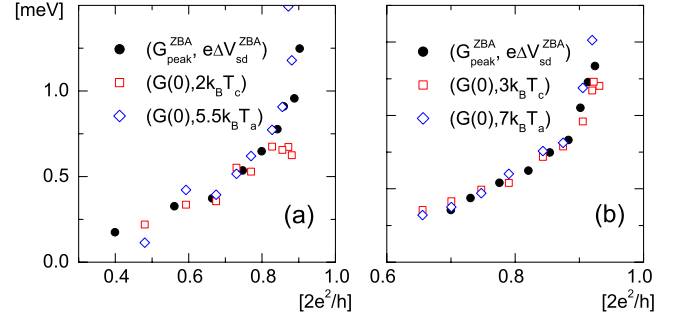


FIG. 5. (Color online)  $(G_{peak}^{ZBA}, e\Delta V_{sd}^{ZBA})$ ,  $[G(0), \text{scaled } T_c]$ , and  $[G(0), \text{scaled } T_a]$  on the same plot for two  $L$ =quasizero QWs.

two  $L$ =quasizero QWs.  $G_{peak}^{ZBA}$  is the conductance at the ZBA peak at the base temperature. In Fig. 5(a), three traces of  $[G(0), 2k_B T_c]$ ,  $[G(0), 5.5k_B T_a]$ , and  $(G_{peak}^{ZBA}, e\Delta V_{sd}^{ZBA})$  collapse onto one curve for one sample. Likewise in Fig. 5(b), three traces of  $[G(0), 3k_B T_c]$ ,  $[G(0), 7k_B T_a]$ , and  $(G_{peak}^{ZBA}, e\Delta V_{sd}^{ZBA})$  collapse also onto one curve for the other sample. Although the factors are slightly different, the scenario is robust. Three characteristic quantities,  $T_c$ ,  $T_a$ , and  $\Delta V_{sd}^{ZBA}$ , decrease monotonically with decreasing zero-bias differential conductance.

While the 0.7 anomaly manifests at high temperatures, it is also observable at finite source-drain biases at low temperatures, seen as bunches of curves, e.g., for  $|V_{sd}| \geq 0.6$  mV in Figs. 3(a) and 3(b). For a specific  $V_{sg}$ , increasing  $|V_{sd}|$  from zero-bias reduces the conductance while the relation of  $G$  versus  $V_{sd}$  forms the ZBA. The fact that the three traces obtained from two different measurements match suggests that the temperature- and bias-induced conductance reductions are strongly correlated.

Theoretical works suggested that conductance decreases with increasing energy scale (either bias voltage or temperature) under the consideration of backscattering.<sup>35,36</sup> Increasing either the bias or temperature enlarges the momentum space of integration and henceforth increases backscattered current or resistance. Calculations showed that multiple-electron backscattering becomes frequent as the source-drain bias increases, leading to a reduced conductance, manifesting as ZBA, whereas enhanced EEI prompts strong multiple-electron scattering to weaken the ZBA.<sup>35,37</sup> On the other hand, several groups have suggested that electron-electron scattering brings about a reduced conductance at elevated temperatures.<sup>16,35,37–40</sup> The temperature-induced conductance correction was suggested to follow an activation law.<sup>38</sup> Thermal-activated dependence of conductance can also be predicted by taking the backscattering of electrons mediated by acoustic phonons into account.<sup>36</sup> The same mechanism can describe the negative correction to conductance by the finite source-drain bias in ZBA as well. The theoretical proposals provide a picture that electron backscattering results in ZBA and temperature-dependent conductance, which may explain our results.

Comparing the spectroscopies reported in Refs. 4, 22, 23, 32, and 41, the shape, amplitude, and width of the ZBA

varied from sample to sample with different 2DEG and device structures. This variability implies that the details of local potential profiles, electric fields, and intrinsic 2DEG properties which affect microscopic electron scattering are important for the characteristics of the ZBA and temperature dependence of conductance. These observations are consistent with our report.

#### IV. SUMMARY

We provide evidence that ZBA depends systematically on physical properties of QWs. The amplitude and width of the ZBA decrease with either decreasing carrier density or increasing channel length, wherein the scattering rate of electrons is expected to increase. The ZBA is totally suppressed by strong scattering, in a either very low carrier density or long QW. The activation model is preferable for describing

the temperature-dependent conductance reduction. Moreover, the conductance dependence on temperature departs from the activation model at a cutoff. Scaling of the cut-off energy, activation energy, and ZBA width indicates that the temperature- and bias-induced conductance reductions are affected by the same physics. Theoretical predictions taking electron backscattering into account are in accordance with our results. We believe that electron scattering has a central role in our observations.

#### ACKNOWLEDGMENTS

We have benefited from discussions with C. S. Chu, J. H. Hsiao, P. J. Lin, and L. Y. Wang. We thank J. M. Valles, Jr. for a critical reading of the manuscript. This work was supported by NSC grant in Taiwan under Project No. NSC96-2112-M-009-030-MY3 and MOE ATU program.

- 
- <sup>1</sup>D. A. Wharam, T. J. Thornton, R. Newbury, M. Pepper, H. Ahmed, J. E. F. Frost, D. G. Hasko, D. C. Peacock, D. A. Ritchie, and G. A. C. Jones, *J. Phys. C* **21**, L209 (1988).
- <sup>2</sup>B. J. van Wees, H. van Houten, C. W. J. Beenakker, J. G. Williamson, L. P. Kouwenhoven, D. van der Marel, and C. T. Foxon, *Phys. Rev. Lett.* **60**, 848 (1988).
- <sup>3</sup>K. J. Thomas, J. T. Nicholls, M. Y. Simmons, M. Pepper, D. R. Mace, and D. A. Ritchie, *Phys. Rev. Lett.* **77**, 135 (1996).
- <sup>4</sup>S. M. Cronenwett, H. J. Lynch, D. Goldhaber-Gordon, L. P. Kouwenhoven, C. M. Marcus, K. Hirose, N. S. Wingreen, and V. Umansky, *Phys. Rev. Lett.* **88**, 226805 (2002).
- <sup>5</sup>R. Akis and D. K. Ferry, *J. Phys.: Condens. Matter* **20**, 164201 (2008).
- <sup>6</sup>A. A. Starikov, I. I. Yakimenko, and K. F. Berggren, *Phys. Rev. B* **67**, 235319 (2003).
- <sup>7</sup>K. F. Berggren and I. I. Yakimenko, *Phys. Rev. B* **66**, 085323 (2002).
- <sup>8</sup>P. Jaksch, I. Yakimenko, and K. F. Berggren, *Phys. Rev. B* **74**, 235320 (2006).
- <sup>9</sup>A. Lassl, P. Schlagheck, and K. Richter, *Phys. Rev. B* **75**, 045346 (2007).
- <sup>10</sup>P. Havu, M. J. Puska, R. M. Nieminen, and V. Havu, *Phys. Rev. B* **70**, 233308 (2004).
- <sup>11</sup>D. J. Reilly, G. R. Facer, A. S. Dzurak, B. E. Kane, P. J. Stiles, R. G. Clark, A. R. Hamilton, J. L. O'Brien, N. E. Lumpkin, L. N. Pfeiffer, and K. W. West, *Phys. Rev. B* **63**, 121311(R) (2001).
- <sup>12</sup>D. J. Reilly, T. M. Buehler, J. L. O'Brien, A. R. Hamilton, A. S. Dzurak, R. G. Clark, B. E. Kane, L. N. Pfeiffer, and K. W. West, *Phys. Rev. Lett.* **89**, 246801 (2002).
- <sup>13</sup>D. J. Reilly, *Phys. Rev. B* **72**, 033309 (2005).
- <sup>14</sup>Y. Tokura and A. Khaetskii, *Physica E* **12**, 711 (2002).
- <sup>15</sup>K. A. Matveev, *Phys. Rev. B* **70**, 245319 (2004).
- <sup>16</sup>K. A. Matveev, *Phys. Rev. Lett.* **92**, 106801 (2004).
- <sup>17</sup>Y. Meir, K. Hirose, and N. S. Wingreen, *Phys. Rev. Lett.* **89**, 196802 (2002).
- <sup>18</sup>K. Hirose, Y. Meir, and N. S. Wingreen, *Phys. Rev. Lett.* **90**, 026804 (2003).
- <sup>19</sup>T. Rejec and Y. Meir, *Nature (London)* **442**, 900 (2006).
- <sup>20</sup>J. H. Hsiao, K. M. Liu, S. Y. Hsu, and T. M. Hong, *Phys. Rev. B* **79**, 033304 (2009).
- <sup>21</sup>F. Sfigakis, C. J. B. Ford, M. Pepper, M. Kataoka, D. A. Ritchie, and M. Y. Simmons, *Phys. Rev. Lett.* **100**, 026807 (2008).
- <sup>22</sup>T. M. Chen, A. C. Graham, M. Pepper, I. Farrer, and D. A. Ritchie, *Phys. Rev. B* **79**, 153303 (2009).
- <sup>23</sup>S. Sarkozy, F. Sfigakis, K. Das Gupta, I. Farrer, D. A. Ritchie, G. A. C. Jones, and M. Pepper, *Phys. Rev. B* **79**, 161307(R) (2009).
- <sup>24</sup>D. Hartmann, L. Worschech, and A. Forchel, *Phys. Rev. B* **78**, 113306 (2008).
- <sup>25</sup>K. J. Thomas, J. T. Nicholls, M. Pepper, W. R. Tribe, M. Y. Simmons, and D. A. Ritchie, *Phys. Rev. B* **61**, R13365 (2000).
- <sup>26</sup>B. E. Kane, G. R. Facer, A. S. Dzurak, N. E. Lumpkin, R. G. Clark, L. N. Pfeiffer, and K. W. West, *Appl. Phys. Lett.* **72**, 3506 (1998).
- <sup>27</sup>K. M. Liu, H. I. Lin, V. Umansky, and S. Y. Hsu, *Physica E* **42**, 1122 (2010).
- <sup>28</sup>L. Martin-Moreno, J. T. Nicholls, N. K. Patel, and M. Pepper, *J. Phys.: Condens. Matter* **4**, 1323 (1992).
- <sup>29</sup>B. L. Altshuler and A. G. Aronov, *Sov. Phys. JETP* **48**, 812 (1979).
- <sup>30</sup>T. Morimoto, M. Henmi, R. Naito, K. Tsubaki, N. Aoki, J. P. Bird, and Y. Ochiai, *Phys. Rev. Lett.* **97**, 096801 (2006).
- <sup>31</sup>E. J. Koop, A. I. Lerescu, J. Liu, B. J. van Wees, D. Reuter, A. D. Wieck, and C. H. van der Wal, *J. Supercond. Nov. Magn.* **20**, 433 (2007).
- <sup>32</sup>A. Kristensen, H. Bruus, A. E. Hansen, J. B. Jensen, P. E. Lindelof, C. J. Marckmann, J. Nygård, C. B. Sørensen, F. Beuscher, A. Forchel, and M. Michel, *Phys. Rev. B* **62**, 10950 (2000).
- <sup>33</sup>H. Bruus, V. Cheianov, and K. Flensberg, *Physica E* **10**, 97 (2001).
- <sup>34</sup>The Kondo-type model for a quantum wire:  $G_{KL}(T) = G(0)[1/\{2[1+(2^{1/s}-1)(T/T_{KL})^2]^{-s}\}+1/2]$ , where  $s=0.22$ . Although numerical fit using this model can describe part of data, there is no systematic relation between the fitting parameter  $T_{KL}$

and split gate voltage.

- <sup>35</sup>A. M. Lunde, A. De Martino, A. Schulz, R. Egger, and K. Flensberg, *New J. Phys.* **11**, 023031 (2009).
- <sup>36</sup>G. Seelig and K. A. Matveev, *Phys. Rev. Lett.* **90**, 176804 (2003).
- <sup>37</sup>D. Meidan and Y. Oreg, *Phys. Rev. B* **72**, 121312(R) (2005).
- <sup>38</sup>A. M. Lunde, K. Flensberg, and L. I. Glazman, *Phys. Rev. B* **75**, 245418 (2007).
- <sup>39</sup>D. Schmeltzer, A. Saxena, A. R. Bishop, and D. L. Smith, *Phys. Rev. B* **71**, 045429 (2005).
- <sup>40</sup>J. Rech and K. A. Matveev, *Phys. Rev. Lett.* **100**, 066407 (2008).
- <sup>41</sup>J. C. Chen, Y. Lin, K. T. Lin, T. Ueda, and S. Komiyama, *Appl. Phys. Lett.* **94**, 012105 (2009).